

The value of Micro-CT in the detection of nicotine induced alveolar bone osteogenesis and microstructure in rats

X. Li^{1,2*}, J. Mi^{1,2}, Y. Zhang^{1,2}

¹Department of Caries and Endodontics, Tianjin Stomatological Hospital, School of Medicine, Nankai University, Tianjin 300041, China

²Tianjin Key Laboratory of Oral and Maxillofacial Function Reconstruction & Stomatology Institute of Nankai University, Tianjin 300041, China

► Original article

ABSTRACT

*Corresponding author:

Xinming Li, M.D.,

E-mail: dlxm19921fs@163.com

Received: May 2025

Final revised: September 2025

Accepted: October 2025

Int. J. Radiat. Res., April 2026;
24(2): 405-410

DOI: 10.61186/ijrr.24.2.15

Background: Explore the effects of different concentrations of nicotine on the microstructure of rat alveolar bone and the expression of osteogenic related proteins, in order to clarify its role in alveolar bone osteogenic metabolism. **Materials and Methods:** In this study, 28 8-week-old male Sprague Dawley (SD) rats were randomly divided into four groups (control group, low-dose group, medium dose group, high-dose group) and subjected to continuous intraperitoneal injection intervention for 180 days. Subsequently, the microstructure characteristics of alveolar bone were analyzed using micro computed tomography (Micro-CT), and the expression of osteogenic related proteins was accurately determined by combining immunohistochemistry and qRT PCR techniques. **Results:** Nicotine dose dependently reduces the volume of rat alveolar bone and damages its microstructure; Nicotine dose dependently reduces the expression of type I collagen (COL-I), alkaline phosphatase (ALP), osteocalcin (OCN), and bone sialoprotein (BSP), while increasing the expression of osteopontin (OPN). **Conclusion:** Nicotine interferes with the osteogenic process of rat alveolar bone by affecting the expression of osteogenic related proteins.

Keywords: Nicotine, alveolar bone, osteogenesis-related proteins, microstructure.

INTRODUCTION

Smoking is a serious public health problem worldwide, with approximately 6 million deaths per year ⁽¹⁾. It is estimated that China has over 300 million smokers, ranking first in the world. Smoking is a major risk factor for oral diseases, as well as bone metabolism disorders such as osteoporosis and osteoarthritis ⁽²⁻⁴⁾. Passive smoking in pregnant rats lags the development of dental embryos and alveolar bone and suppresses mineralization levels in fetal rats ⁽⁵⁾, which confirms that smoking has an important regulatory effect on bone metabolism.

Nicotine, as the main toxic component of tobacco ⁽⁶⁾, has been confirmed by multiple studies to have adverse effects on bone metabolism. For example, some studies have shown that exposure to nicotine after tibial osteotomy significantly increases the risk of poor bone healing and delays the process of fracture healing ^(7,8). High concentrations of nicotine can inhibit bone metabolism and collagen synthesis ⁽⁹⁾. The alveolar bone is an important tooth-supporting tissue and is the most metabolically active area of the skeletal system of the body, making it particularly sensitive to external stimuli. Research has shown that nicotine can reduce calcium and phosphorus deposition ⁽¹⁰⁾, inhibit the expression of bone morphogenetic proteins in alveolar bone ⁽¹¹⁾, and after intraperitoneal injection of nicotine in SD

rats, nicotine deposition proportional to the injection amount can be detected in alveolar bone and teeth, indicating its direct effect on alveolar bone ⁽¹²⁾; In addition, nicotine can disrupt the dynamic balance between osteogenesis and osteoclastogenesis by inhibiting the expression of osteoprotegerin (OPG) ^(13, 14), leading to decreased bone mass and microstructural damage. The early signals of bone metabolism disorders are often reflected in changes in bone microstructure ⁽¹⁵⁾, and osteogenic proteins secreted by osteoblasts such as COL-I and ALP are key substances that maintain normal osteogenic processes ⁽¹⁶⁻¹⁸⁾. In this context, Micro-CT can accurately capture subtle changes in bone mineral density (BMD) and bone microstructure parameters ⁽¹⁹⁾, providing reliable technical support for early assessment of bone microstructure.

This study established SD rat models exposed to different concentrations of nicotine through intraperitoneal injection, and quantitatively analyzed the microstructural changes of alveolar bone using Micro-CT. The expression of osteogenic related proteins was systematically detected at the mRNA and protein levels to clarify the dose-dependent effects and potential mechanisms of nicotine on alveolar bone osteogenic metabolism. This provides a more comprehensive experimental basis for revealing the role of nicotine in regulating alveolar bone osteogenesis.

MATERIALS AND METHODS

Animal model

Prepare 28 8-week-old male SPF grade SD rats weighing approximately 230 g (provided by the Animal Experiment Center of Sichuan University). The feeding conditions were temperature 25°C, humidity 50%, standard pellet feed was used, and the room was well ventilated with sufficient natural light. After one week of acclimatization, the rats were numbered with picric acid and randomly divided into four groups (n = 7): control group (saline), low-dose group (1.6 mg/kg nicotine), medium-dose group (3.2 mg/kg nicotine), and high-dose group (4.8 mg/kg nicotine). Saline and nicotine solution were all administrated through intraperitoneal injection. The injection operators were unified to ensure the consistency of operation. After 180 consecutive days of intraperitoneal injection, Rats were anesthetized and euthanized with chloral hydrate (Sichuan Wicker Biotech, China), the mandibles of rats were taken bilaterally, the soft tissues were trimmed and removed, and only the alveolar bone of the molar region was preserved, the left alveolar bone was placed in 4% paraformaldehyde for micro-CT detection, and then joint sections of the dentition and periodontal region were made for hematoxylin-eosin (HE) staining and immunohistochemistry experiments, and the right alveolar bone was frozen in liquid nitrogen immediately after removal.

HE staining

Place the fixed tissue into melted paraffin and use a slicer to slice the paraffin blocks into thin slices 5 µm thick, then dehydrated with ethanol (Wuhan Smaike, China) and xylene (Hubei Taikang, China), then stained with hematoxylin solution (Biyuntian, China) for 5 min, and washed off with running water to remove the hematoxylin solution for 10 s. The stained samples were differentiated in 1% HCl-ethanol for 5 s. The samples were stained with 0.5% eosin for 30 s. After rinsing and dehydration, seal the slide. Finally, place the sealed film under a microscope for observation.

Micro-CT scanning

The left alveolar bone was fixed in 4% paraformaldehyde. The fixed alveolar bone was fixed in foam and scanned with micro-CT instrument (Micro CT HiscanXM, China). The scanning voltage is 70 kV, the current is 114 µA, the accuracy is 10 µm, and a pixel of 1024 × 1024 for about 26 min. After scanning, the micro-CT software was used to reconstruct the three-dimensional images and analyze the region of interest (ROI), including BMD, bone volume/tissue volume (BV/TV), connectivity density (Conn.D), trabecular number (Tb.N), trabecular thickness (Tb.Th), and trabecular

separation (Tb.Sp).

qRT-PCR

Take alveolar bone samples from each group of rats and extract total RNA using a standard TRIzol kit (Invitrogen, USA). Using purified total RNA as a template, cDNA first strand synthesis was performed using a reverse transcription kit (Fermentas, Lithuania). The specific operation process is as follows: mixing 25 µl 2×PCR buffer, 1µl upstream and downstream primers (Sangon Biotech, China), 0.5 µl of Sybr green I (Bimake, USA), 2 µl cDNA sample, and 20.5 µl diethypyrocarbonate (DEPC) water (Sigma, USA) for qRT-PCR amplification and data analysis. The primers used in these studies are listed in table 1.

Table 1. The primer sequences of COL-I, ALP, OCN, BSP, OPN, and ACTB.

Genes	Primer sequences
COL-I	F: GCTGGCAAGAATGGCGAC
	R: AAGCCACGATGACCCTTTATG
ALP	F: GTCTGGAGTCAGGCTGGATAGTC
	R: AGGCGAGTCACTGCTGGG
OCN	F: GGAGGGCAGTAAGGTGGTGA
	R: ACGGTGGTGCCATAGATGC
BSP	F: CGAGGAGGCAAGCGTCAC
	R: ACCGTGCTGCTCTTTCTGG
OPN	F: AACAGTATCCCGATGCCACA
	R: TGGCTGGTCTTCCCGTTG
ACTB	F: CCCATCTATGAGGGTTACGC
	R: TTTAATGTACGCACGATTC

Immunohistochemistry

After fixing the sample, embed it in paraffin and cut it into 5 µm sections. Firstly, pre-processing is carried out, followed by dewaxing, dehydration, antigen retrieval, and rinsing. Then incubate at room temperature with 3% H₂O₂ for 15 min; Incubate the slices overnight with the following primary antibodies at 4°C - COL-I (1: 75, Wuhan Sanying, China), ALP (1: 200, Wuhan Sanying, China), OCN (1: 75, R&D Systems, USA), BSP (1: 400, Beijing Bo Aosun, China), OPN (1: 100, Novus, USA); After washing the slices with phosphate buffered saline (PBS), add the secondary antibody (1:1, DaKo, Denmark) and incubate at room temperature for 45 min; After rinsing, add 3,3-diaminobenzidine (DAB) for color development, then counterstain with hematoxylin for 3 min. After rinsing and dehydration, seal the slide. Finally, place the sealed film under a microscope for observation.

Statistics and analysis

Perform one-way ANOVA using SPSS17.0 software. IPP6.0 software was used to collect the average optical density values of alveolar bone immunohistochemistry under a 400× light microscope. P<0.05 indicates statistical significance of the difference.

RESULTS

Effect of nicotine on periodontal tissues

Periodontal tissue includes gingiva, periodontal membrane, alveolar bone and osteoid. Periodontal tissue is an important supporting tissue of teeth, and its injury can cause deep periodontal pocket, attachment loss, alveolar bone absorption, and finally loosen and fall out of teeth⁽²⁰⁾. As shown in figure 1, in the control group, the periodontal membrane fibers were neatly arranged, the alveolar bone trabeculae were thick and dense, and the bone marrow cavity gap was small. In the low-dose nicotine group, there was no obvious abnormality in periodontal fiber arrangement, a small amount of inflammatory cell infiltration, no obvious abnormality in trabecular structure, and a slight increase in bone marrow space. In the nicotine medium dose group, periodontal fiber arrangement was obviously disordered, periodontal space widened, inflammatory cell infiltration increased, bone trabecular shape was sparse and curved, and bone marrow space was larger. In the high-dose nicotine group, the periodontal membrane fibers were sparse, the arrangement was seriously disordered, the periodontal space was widened, the inflammatory cell infiltration was increased, the bone trabecula was sparse and curved, the bone marrow space was significantly enlarged, and bone resorption was intensified. Thus, we found that nicotine can cause abnormal changes in periodontal tissue structure.

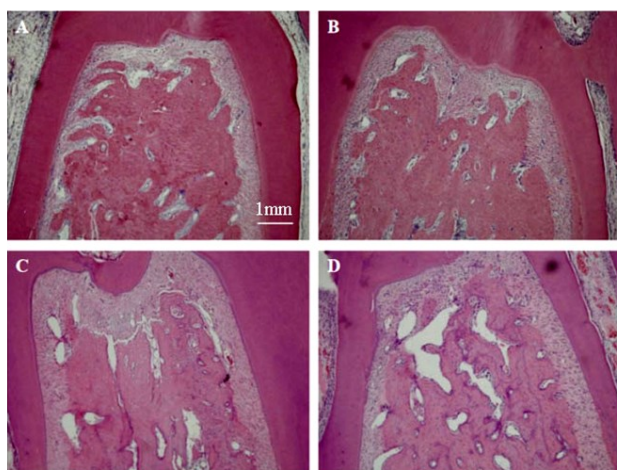


Figure 1. Photomicrographs showing H&E-stained periodontal tissue from rats exposed to varying nicotine doses, demonstrating disordered fibers, widened periodontal space, increased inflammation, reduced BMD and other abnormalities that worsen with higher nicotine dose compared to the control group. Four images labeled A to D show: **A)** Control group with neat fibers **B)** Low nicotine dose with minimal changes **C)** Medium nicotine dose showing moderate fiber disorder and bone loss **D)** High nicotine dose with severe abnormalities.

Effect of nicotine on the microstructure of alveolar bone

The results of our study (figure 1) have confirmed

that the nicotine intervention group had varying degrees of increased bone marrow cavity space and disorganization of bone trabeculae and other structures, suggesting that there may be a decrease in bone mass due to bone resorption and damage to the alveolar bone microarchitecture. BMD is a common parameter reflecting bone mass⁽²¹⁾. Bone microstructure is a general term for the three-dimensional configuration of bone trabeculae and the degree of connection between trabeculae. The change of bone microstructure may be the early manifestation of a variety of bone metabolic imbalance diseases⁽²²⁾. Micro-CT can accurately detect changes in BMD and bone microstructural parameters⁽²³⁾, and its main parameters for evaluating bone microstructure include BV/TV, Conn.D, Tb.N, Tb.Th, Tb.Sp, etc. Therefore, we used Micro-CT to quantitatively analyze the BMD and microstructure of alveolar bone in SD rats to clarify the effects of different concentrations of nicotine on the BMD and microstructure of alveolar bone.

Inside the alveolar bone between the roots of the mandibular first molar on the left side of SD rats were used as ROI⁽²⁴⁾, which is commonly used for trabecular bone morphology due to the presence of a significant stress concentration in this region. Micro-CT 3D reconstruction images of alveolar bone showed that there was no significant change in alveolar bone height and root exposure at low nicotine doses. However, when nicotine dosage was 4.8 mg/kg, alveolar bone height significantly decreased and the root was partially exposed (figure 2).

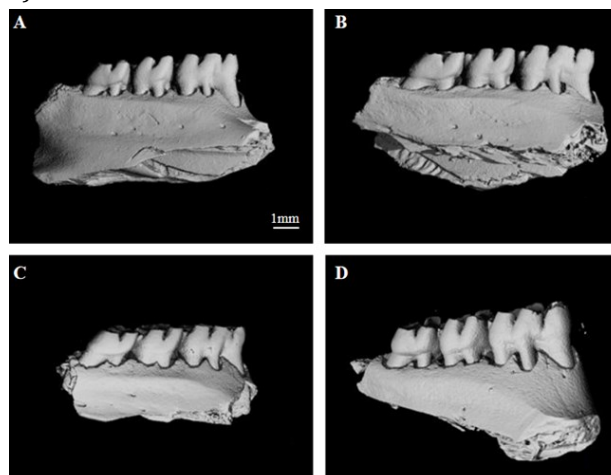


Figure 2. 3D micro-CT reconstructions of alveolar bone from rats exposed to varying nicotine doses, focused on the ROI between mandibular first molar roots. Images show minimal changes to bone height and root exposure in low and medium dose groups compared to control. The high dose group demonstrates significantly reduced bone height and partial root exposure indicating bone resorption. Four images labeled A to D show: **A)** Control group **B)** Low dose nicotine with no significant changes **C)** Medium dose nicotine with no significant changes **D)** High dose nicotine showing reduced bone height and exposed roots.

Subsequently, the alveolar bone ROI of SD rats was determined in each group to assess the BMD data. As shown in figure 3, BMD decreased progressively with increasing nicotine concentration, and the difference between the medium dose and high dose groups was significant ($P < 0.05$). Additionally, nicotine reduced BV/TV and Tb.N in the

alveolar bone of SD rats, while increasing Tb.Sp. Therefore, our study demonstrated that nicotine could reduce the bone mass and destroy the bone microstructure of the alveolar bone, which in turn affected the bone metabolic homeostasis of the alveolar bone.

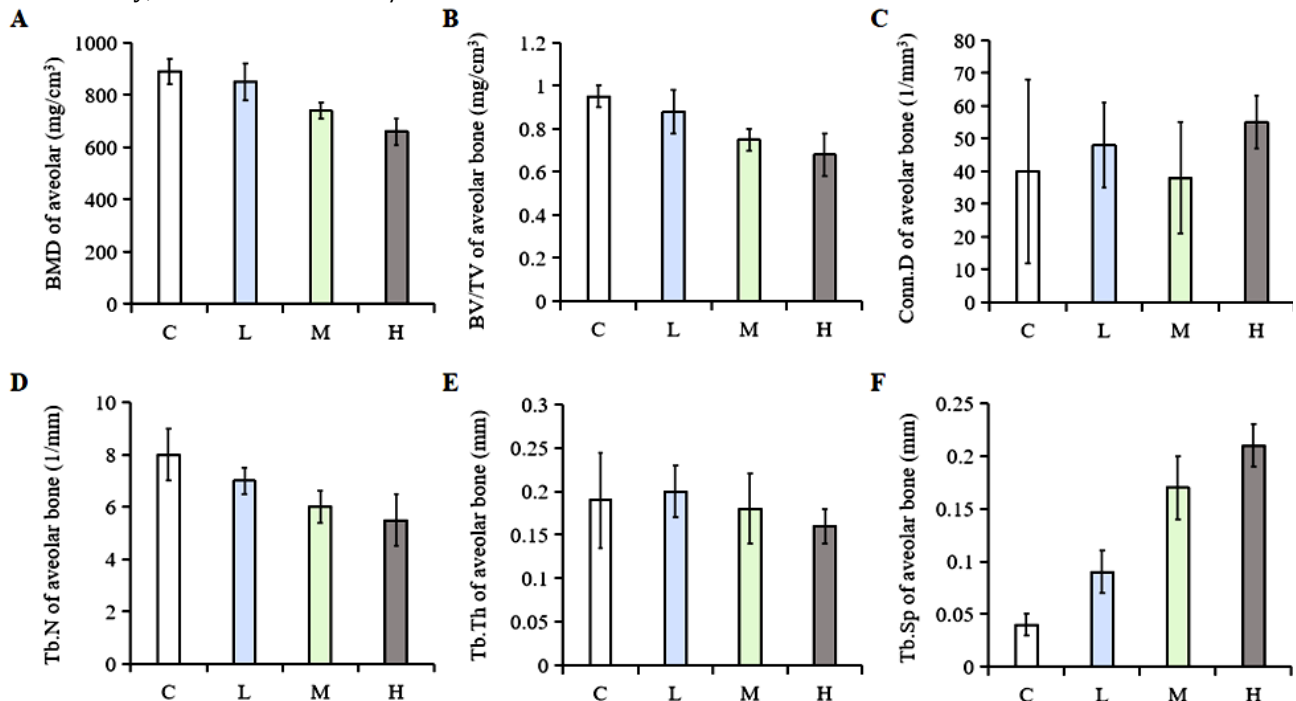


Figure 3. Bar charts showing effects of nicotine dose on alveolar BMD and microstructure in rats. Graph A demonstrates decreasing BMD with increasing nicotine dose. Figure B, D and F show nicotine reduces BV/TV ratio, Tb.N, and increases Tb.Sp compared to control. Graphs C and E show no significant difference in Conn.D and Tb.Th. (C: control group, L: low-dose group, M: medium-dose group, H: high-dose group).

Effects of nicotine on the expression of osteogenesis-related genes

Osteogenic proteins are involved in the process of osteogenesis, so we further studied the expression of transcription and translation of osteogenic genes. The mRNA expression of COL-I, ALP, OCN, BSP, and OPN was analyzed (figure 4), and the results showed that as the nicotine dose increased, the mRNA levels of COL-I, ALP, and OCN gradually decreased, but the expression level of BSP did not change significantly, while the expression level of OPN increased to a certain extent. This indicates that nicotine can inhibit the expression of *col-1*, *alp*, *ocn* genes, but has no effect on *bsp* genes, in addition, nicotine can increase the level of *opn* mRNA, and this regulatory effect with the increase in nicotine concentration and increase.

Effects of nicotine on the expression of osteogenesis-related proteins

Osteogenesis-related proteins play an important regulatory role in the process of osteogenesis. These proteins can be categorized into two groups, one is collagen, mainly COL-I, and the other is non-collagenous proteins, which are secreted by osteoblasts and transferred to the extracellular matrix to play their roles, including ALP, OCN, BSP,

OPN, etc. The study showed (figure 5) that with the increase of nicotine dose, the brown positive expression areas of COL-I, ALP, OCN, and BSP decreased and their expression decreased, but the positive expression of OPN increased and its expression increased. In summary, nicotine can inhibit the protein expression of COL-I, ALP, OCN, and BSP, while promoting the protein expression of OPN.

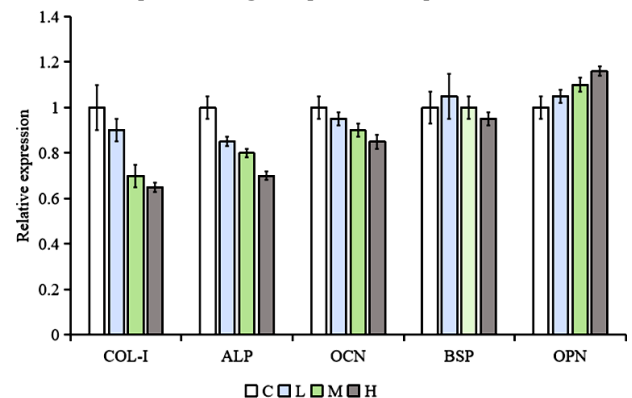


Figure 4. The bar chart displays the mRNA expression of COL-I, ALP, OCN, BSP, and OPN in the alveolar bone of nicotine exposed rats. As the nicotine dosage increases, the levels of COL-I, ALP, and OCN gradually decrease; There was no significant difference in bone sialoprotein BSP among the groups; The expression of OPN increases in a dose-dependent manner with the increase of nicotine dose.

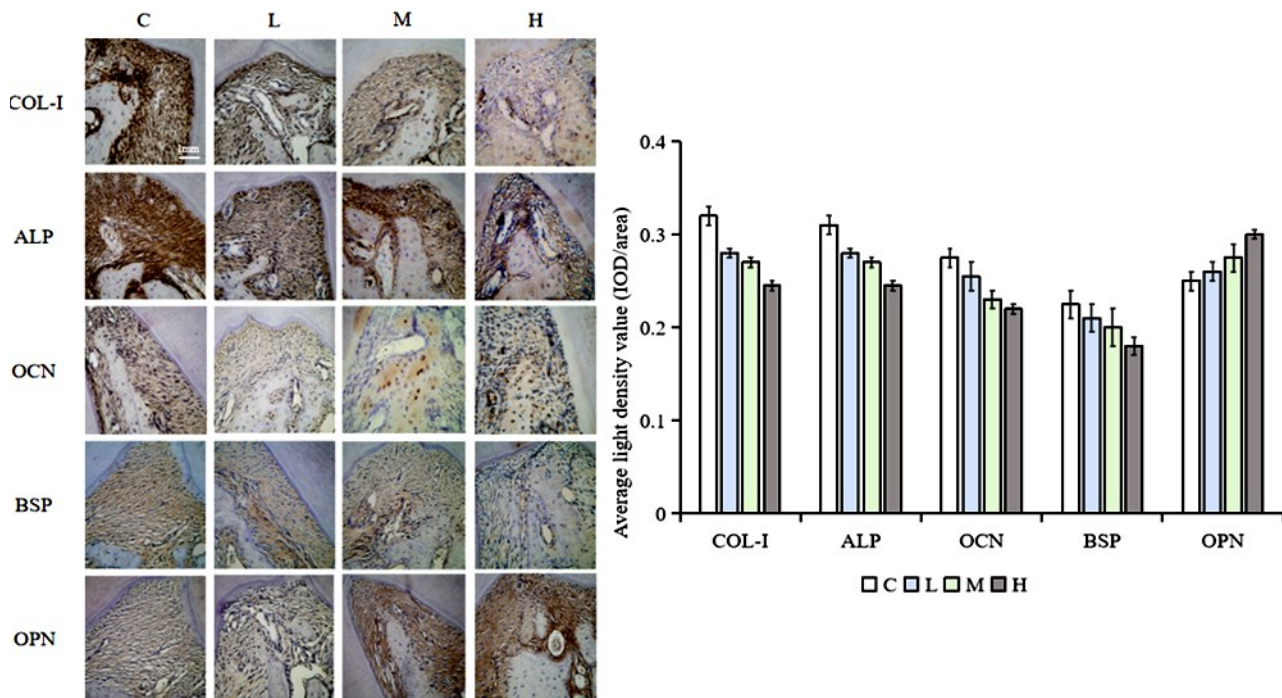


Figure 5. Photomicrographs showing immunohistochemical staining for osteogenic proteins in alveolar bone from nicotine-exposed rats. Images demonstrate decreased brown staining indicating reduced expression of collagen I, alkaline phosphatase, OCN, and BSP compared to control. OPN expression appears increased in the high nicotine dose group. Charts showing quantitative optical density values confirm significant decreases in collagen I, alkaline phosphatase, OCN and BSP, and an increase in OPN, with high nicotine exposure.

DISCUSSION

Our study evaluated the effects of different concentrations of nicotine on periodontal tissues, alveolar bone microstructure, and expression of osteogenesis-related proteins in SD rats through histopathological, morphological, and molecular biological experiments, and preliminarily investigated the effects of nicotine on alveolar bone osteogenesis and possible mechanisms. This study indicates that nicotine damages the microstructure of periodontal tissue and alveolar bone in SD rats in a dose-dependent manner, and interferes with osteogenic metabolism by regulating the expression of osteogenic related proteins. This may be related to nicotine upregulating inflammatory factors such as IL-1 β , IL-6, TNF - α (25), synergistically reducing periodontal ligament cell activity with bacterial lipopolysaccharides in the gingival sulcus (26), and promoting osteoclast secretion of H+ to accelerate bone resorption (27). From a mechanistic perspective, nicotine inhibition of COL-I, ALP, and OCN may weaken bone matrix construction and mineralization processes (28), while upregulation of OPN may inhibit bone calcification through changes in its phosphorylation status (29), collectively leading to bone loss and structural damage.

The alveolar bone resorption and poor bone microstructure observed in the present study may be related to nicotine-induced down-regulation of COL-I, ALP, and OCN, thereby affecting alveolar bone osteogenesis and metabolism, which is in line with

the results of previous studies (30,31). Highly phosphorylated OPN may bind to HA and form inactive OPN-HA structures, thereby reducing the amount of active HA in the calcification zone and thus inhibiting bone formation (32). We speculate that highly phosphorylated OPN may dominate rat alveolar bone under nicotine intervention, thus inhibiting the osteogenic process, which may be one of the important reasons why nicotine affects the osteogenic metabolism of alveolar bone. The specific mechanism by which nicotine affects alveolar bone osteogenic metabolism was not further explored in this study, and further experiments need to be designed to elucidate it.

In summary, for cancer patients receiving radiotherapy, radiotherapy itself can easily cause radiation damage to the alveolar bone, manifested as decreased osteogenic function and destruction of bone microstructure (33). Nicotine further inhibits osteogenic associated proteins and exacerbates bone structure damage, thereby increasing the risk of radiation-induced osteonecrosis, tooth loosening, and other conditions. Therefore, in clinical practice, it should be emphasized that such patients should quit smoking to reduce the cumulative damage of nicotine to alveolar bone, improve bone repair and oral function prognosis after radiotherapy.

Acknowledgment: Not Applicable.

Declarations of interest: No conflict of interest has been declared by the authors.

Funding: This work was sponsored by Tianjin Health

Research Project (Grant No.TJWJ2024QN073).

Ethical consideration: This study was approved by the Ethics Committee of School of Medicine, Nankai University.

Author contribution: X.L: Conceptualization, Project administration, Investigation, Data curation, Writing - original draft, Writing - review & editing, Fundig acquisition. J.M: Investigation, Data curation. Y.Z.: Data curation, Supervision. All authors have approved **Data Availability Statement:** The data that support the findings of this study are available on 10.6084/m9.figshare.25051568.

REFERENCES

- Durojaye E (2018) The WHO tobacco convention: A new dawn in the implementation of international health instrument? Comment on "the legal strength of international health instruments - what it brings to global health governance?". *Int J Health Policy Manag*, **7** (2): 189-191.
- Jeong SM, Yoo JE, Park, JunheeJung, WonyoungLee, Kyu NaHan, *et al.* (2023) Smoking behavior change and risk of cardiovascular disease incidence and mortality in patients with type 2 diabetes mellitus. *Cardiovasc Diabetol*, **22**(1): 193.
- Marruganti C, Romandini M, Gaeta C, Cagidiaco EF, Discepoli N, Parrini S, *et al.* (2023) Healthy lifestyles are associated with a better response to periodontal therapy: A prospective cohort study. *J Clin Periodontol*, **50**(8): 1089-1100.
- Peng Q, Duan N, Wang X, Wang W (2023) The potential roles of cigarette smoke-induced extracellular vesicles in oral leukoplakia. *Eur J Med Res*, **28**(1): 250.
- VVivarelli F, Granata S, Rullo L, Mussoni M, Candeletti S, Romualdi P, *et al.* (2022) On the toxicity of e-cigarettes consumption: Focus on pathological cellular mechanisms. *Pharmacol Res*, **182**: 106315.
- Montjean D, Godin Pagé, Marie-Hélène, Bélanger, Marie-Claire, Benkhalifa M, *et al.* (2023) An overview of e-cigarette impact on reproductive health. *Life (Basel)*, **13**(3): 827.
- Arnez MFM, Monteiro PM, Paula-Silva FWG, Dessotti GB, Menezes LM, Küchler EC, *et al.* (2022) Impact of cigarette smoke on osteogenic and osteoclast signaling in middle palatal suture. *Braz Dent J*, **33**(2): 99-108.
- Takeshita A, Shimamoto H, Uchimoto Y, Tsujimoto T, Miyamoto T, Kreiborg S, *et al.* (2023) High-dose-rate mold brachytherapy for mandibular gingival squamous cell carcinoma in outpatient setting – Initial case report. *Int J Radiat Res*, **21** (4) :849-853
- Shyu JF, Liu WC, Zheng CM, Fang TC, Hou YC, Chang CT, *et al.* (2021) Toxic effects of indoxyl sulfate on osteoclastogenesis and osteoblastogenesis. *Int J Mol Sci*, **22**(20): 11265.
- Hasan WNW, Chin KY, Jolly JJ, Ghafar NA, Soelaiman IN (2018) Identifying potential therapeutics for osteoporosis by exploiting the relationship between mevalonate pathway and bone metabolism. *Endocr Metab Immune Disord Drug Targets*, **18**(5): 450-457.
- Wei X, Liu Q, Liu L, Tian W, Wu Y, Guo S (2023) Periostin plays a key role in maintaining the osteogenic abilities of dental follicle stem cells in the inflammatory microenvironment. *Arch Oral Biol*, **153**: 105737.
- Vimalraj S (2020) Alkaline phosphatase: Structure, expression and its function in bone mineralization. *Gene*, **754**: 144855.
- Cutarelli A, Marini M, Tancredi V, D'Arcangelo G, Murdocca M, Frank C, *et al.* (2016) Adenosine triphosphate stimulates differentiation and mineralization in human osteoblast-like Saos-2 cells. *Dev Growth Differ*, **58**(4): 400-8.
- Gong S, Emperumal CP, Al-Eryani K, Enciso R (2022) Regeneration of temporomandibular joint using in vitro human stem cells: A review. *J Tissue Eng Regen Med*, **16**(7): 591-604.
- Xu XY, Li X, Wang J, He XT, Sun HH, Chen FM (2019) Concise review: Periodontal tissue regeneration using stem cells: Strategies and translational considerations. *Stem Cells Transl Med*, **8**(4): 392-403.
- Pereira LF, Fontes-Pereira AJ, de Albuquerque Pereira WC (2023) Influence of low-intensity pulsed ultrasound parameters on the bone mineral density in rat model: A systematic review. *Ultrasound Med Biol*, **49**(8): 1687-1698.
- Yu Y, Li X, Zheng M, Zhou L, Zhang J, Wang J, *et al.* (2023) The potential benefits and mechanisms of protein nutritional intervention on bone health improvement. *Crit Rev Food Sci Nutr*, **64**(18): 1-15.
- Micheletti C, Jolic M, Grandfield K, Shah FA, Palmquist A (2023) Bone structure and composition in a hyperglycemic, obese, and leptin receptor-deficient rat: Microscale characterization of femur and calvarium. *Bone*, **172**: 116747.
- Iezzi G, Valente NA, Velasco-Ortega E, Piattelli A, Perez A, D'amico E, *et al.* (2023) Alveolar ridge preservation procedures performed with a freeze-dried bone allograft: Histologic outcomes in a cohort study: Part I. *Int J Periodontics Restorative Dent*, **6**: 675-685.
- Liu KH and Hwang SJ (2016) Effect of smoking cessation for 1 year on periodontal biomarkers in gingival crevicular fluid. *J Periodontol Res*, **51**(3): 366-75.
- Huang Q, Ye A, Li P, Bao J, Garfield RE, Liu H (2022) Nicotine ameliorates inflammatory mediators in RU486 induced preterm labor model through activating cholinergic anti-inflammatory pathway. *Cytokine*, **160**: 156054.
- AlQahtani MA, Alayad AS, Alshihri A, Correa FOB, Akram Z (2018) Clinical peri-implant parameters and inflammatory cytokine profile among smokers of cigarette, e-cigarette, and waterpipe. *Clin Implant Dent Relat Res*, **20**(6): 1016-1021.
- Zhang W, Lin H, Zou M, Yuan Q, Huang Z, Pan X, *et al.* (2022) Nicotine in inflammatory diseases: Anti-inflammatory and pro-inflammatory effects. *Front Immunol*, **13**: 826889.
- Elkady A, Kazem H, Elgendy E (2020) Protective effect of vitamin D against rats' mandibular osteoporosis induced by corticosteroids and gamma rays. *Int J Radiat Res*, **18** (1): 125-131.
- Carrillo F, Suter S, Casari FA, Sutter R, Nagy L, Snedeker JG, *et al.* (2020) Digitalization of the IOM: A comprehensive cadaveric study for obtaining three-dimensional models and morphological properties of the forearm's interosseous membrane. *Sci Rep*, **10** (1): 6401.
- Yavas M, Kilitci A, Çelik E, Yegin K, Sirav B, Varol S (2024) Rat brain and testicular tissue effects of radiofrequency radiation exposure: Histopathological, DNA damage of brain and qRT-PCR analysis. *Int J Radiat Res*, **22** (3): 529-536.
- Liang D, Wang KJ, Tang ZQ, Liu RH, Zeng F, Cheng MY, *et al.* (2018) Effects of nicotine on the metabolism and gene expression profile of sprague-dawley rat primary osteoblasts. *Mol Med Rep*, **17**(6): 8269-8281.
- Macdonald HM, Nishiyama KK, Kang J, Hanley DA, Boyd SK (2011) Age-related patterns of trabecular and cortical bone loss differ between sexes and skeletal sites: A population-based HR-pQCT study. *J Bone Miner Res*, **26**(1): 50-62.
- Yucel H, Dundar N, Doguc D, Uguz C, Celik O, Tutku Aksoy F, *et al.* (2022) Evaluation of cognitive functions and EEG records in rats exposed to 2.45 GHz electromagnetic field. *Int J Radiat Res*, **20** (4) :753-760.
- Nicholson T, Scott A, Newton Ede M, Jones SW (2021) The impact of e-cigarette vaping and vapour constituents on bone health. *J Inflamm (Lond)*, **18**(1): 16.
- Gambari L, Grigolo B, Grassi F (2022) Dietary organosulfur compounds: Emerging players in the regulation of bone homeostasis by plant-derived molecules. *Front Endocrinol (Lausanne)*, **13**: 937956.
- Lee SH, Cha JY, Choi SH, Kim BI, Cha JK, Hwang CJ (2021) Effect of nicotine on orthodontic tooth movement and bone remodeling in rats. *Korean J Orthod*, **51**(4): 282-292.
- Hunter GK (2013) Role of osteopontin in modulation of hydroxyapatite formation. *Calcif Tissue Int*, **93**(4): 348-54.